The unoccupied electronic structure of 1T-VSe_2

1990 J. Phys.: Condens. Matter 2 10045

(http://iopscience.iop.org/0953-8984/2/50/009)

J. Phys.: Condens. Matter **2** (1990) 10045–10051. Printed in the UK

The unoccupied electronic structure of 1T-VSe_2

R Claessen, I Schäfer† and M Skibowski
Institut für Experimentalphysik, Universität Kiel, D-2300 Kiel, Federal Republic of Germany

Received 12 June 1990, in final form 14 August 1990

Abstract. By use of angle-resolved inverse photoemission spectroscopy (ARIPES) in the isochromate mode using 9.88 eV photon energy we have studied the unoccupied electronic structure of 1T-VSe_2 along the principal symmetry directions ΓM, ΓM′ and ΓK. The data are found to be in good agreement with the recent ARIPES study of Law *et al* employing 20 eV photon energy. The experimental bands are reasonably well described by band-structure calculations but viewed together with the 20 eV data appear to be less dispersive perpendicular to the surface than theoretically predicted. A structure at 5 eV above E_F for normal incidence can be identified as an image potential state.

1. Introduction

Transition-metal dichalcogenides (TMDCs) continue to be of great interest because of their distinct two-dimensional crystal structure and the occurrence of charge-density waves (CDWs). They consist of hexagonal metal layers sandwiched between chalcogen sheets such that the metal atoms are surrounded by six chalcogen atoms in either octahedral (1T structure) or trigonally prismatic (2H structure) coordination. Among the octahedrally coordinated TMDCs, 1T-VSe_2 is of particular interest because of the extraordinary large trigonal distortion, leading to a c/a ratio of 1.82 (ideal 1T structure, 1.633), reaching almost the value of the 2H structure (1.82–1.85).

The electronic structure of 1T-VSe_2 as described by several band-structure calculations [1–3] consists of bonding (σ) and antibonding (σ^*) bands formed from Se 4p orbitals with some admixture of V 3d and 4p character, while V 3d- derived conduction bands lie in the large $\sigma\sigma^*$ gap of about 7 eV. In the octahedral ligand field the 3d states are split into subbands of t_{2g} (derived from d_{xy}, $d_{x^2-y^2}$ and d_{z^2} orbitals) and e_g (d_{xz}, d_{yz}) symmetry, whose degeneracies become further lifted by the trigonal distortion. The lowest-lying band having largely d_{z^2} character is occupied by one electron, giving rise to the observed metallic behaviour.

While the valence band structure of VSe_2 has been studied by angle-resolved photoemission spectroscopy (ARPES) [4–7] and found to be well described by the band-structure calculations, the V3d states, which are particularly affected by the distortion of the ligand field, are largely empty and hence not accessible by ARPES. However,

† Present address: Philips Medizinsysteme GmbH, Roentgenstrasse 24, D-2000 Hamburg 63, Federal Republic of Germany.

0953-8984/90/5010045 + 07 $03.50

detailed information about the unoccupied band structure can be obtained by angle-resolved *inverse* photoemission spectroscopy (ARIPES). Very recently Law *et al* [8] have published an inverse photoemission study of VSe_2 working at photon energies around 20 eV. In this paper we present ARIPES results along the high-symmetry lines ΓM, ΓM′ and ΓK of the Brillouin zone, utilizing a photon energy of 9.88 eV. We compare our results with the study of Law *et al* and give a contrasting interpretation of a dispersive peak at 5–6 eV above the Fermi level in terms of an image potential state. The experimental conduction band structure derived from our ARIPES data is compared with the *ab initio* band-structure calculation of Zunger and Freeman [2].

2. Experimental details

The ARIPES spectra presented in this work have been obtained in the isochromat mode. The bandpass photon detector operates at a photon energy of 9.88 eV and consists of an open photomultiplier with a CaF_2 entrance window and a KBr-coated photocathode. The low-energy electron source provides a collimated electron beam whose small angular divergence corresponds to a wavevector resolution of better than 0.1 $Å^{-1}$. The spectral sensitivity of the bandpass detector has been measured with synchrotron radiation. The overall spectrometer function as obtained from a convolution of the detector sensitivity and the energy distribution of the electron source has a full width at half-maximum (FWHM) of 640 meV and may be used for numerical deconvolution of the spectra. Further details of the spectrometer have been described elsewhere [9, 10]. The Fermi edge of a clean gold film measured under identical conditions as the sample is used as energy reference.

The work function of VSe_2, which will be of some importance in the discussion of the ARIPES results, has been determined by target-current spectroscopy (TCS) using the ARIPES electron gun. In TCS the current incident on the sample is measured as function of the electron energy. As long as the electron energy is below the vacuum level of the sample surface, zero current is detected until a sharp current onset is observed at the minimum energy where the electrons are able to reach the sample. From this energy and the work function of the electron source it is possible to determine the work function of the sample within an accuracy of ±50 meV. The work function of the electron source cathode can be determined independently by measuring an inverse photoemission spectrum of the Fermi edge of a metal or by elastic reflection of the electron beam into a cylindrical mirror analyzer also present in the vacuum chamber (a complete description of the experimental set-up may be found in [11]). In order to avoid problems arising from the very low kinetic energy of the electrons the sample current onset can be shifted towards higher energies by a negative voltage bias (about 5–10 eV) of the sample. Applying the TCS method to the cleaved surface of VSe_2 single crystals we obtained a work function of 5.76 ± 0.05 eV, which lies within the range of values found for other TMDCs (table 1). However, there appears to be a discrepancy between our result and the value reported by Hughes *et al* [5], who derived a work function of 4.4 eV from the secondary-electron cut-off of their ARPES spectra. It should be noted here that for the case of 1T-TaS_2 [16] we found the work function to be sensitive to a slight surface contamination, resulting in a work function drop as large as 1 eV, which may be a possible explanation of the extraordinary low value of Hughes *et al*.

The 1T-VSe_2 single crystals were prepared from the elements by the iodine vapour transport method. The quality of the crystals was probed by x-ray diffraction applying

Table 1. Work functions of various TMDCs determined with different experimental methods.

Sample	Φ (eV)	Experimental method	Reference
1T-TiS_2	5.92	Kelvin prove	[12]
1T-TiS_2	5.95	TCS	[13]
1T-$TiSe_2$	5.60	TCS	[14]
1T-$TiTe_2$	5.2	Secondary-electron cut-off of ARPES spectra	[15]
1T-TaS_2	5.7	TCS	[16]
1T-VSe_2	5.76	TCS	This work

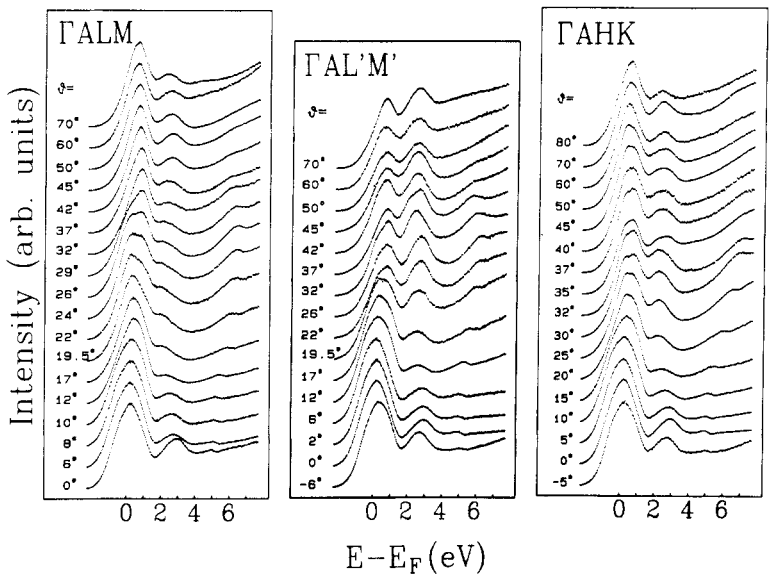

Figure 1. Angle-resolved inverse photoemission spectra of 1T-VSe_2 for three different azimuthal orientations with the electron momentum lying in the ΓALM, ΓAL'M' and ΓAHK half-planes respectively and varying polar angles of incidence.

the Laue method. X-ray diffraction was also used to determine the high-symmetry directions. Comparison of measured and calculated Laue diffraction patterns allowed us to distinguish between the ΓM and ΓM′ directions of the Brillouin zone [17]. The crystals were brought into ultra-high vacuum (about 1×10^{-10} Torr) and cleaved *in situ* perpendicular to the *c* axis. Surface quality and orientation were checked by low-energy electron diffraction (LEED).

3. Experimental conduction band structure

ARIPES has been performed for three different azimuthal orientations which we shall refer to as the ΓM, ΓM′ and ΓK directions, although, strictly speaking, the three-dimensional electron wavevector lies in the ΓALM, ΓAL'M' and ΓAHK half-planes respectively. The corresponding spectra are shown in figure 1. They look very similar to

the data of Law *et al* [1] and also resemble the ARIPES spectra taken from other 1T-TMDCs [15, 16]. They display mainly two features centred at about 1 and 2–3 eV above the Fermi level, which can be attributed to the t_{2g} and e_g manifolds of bands respectively. A third structure located at 5 eV for normal incidence ($\vartheta = 0°$) shows distinct dispersion towards higher energies along ΓM, ΓM′ and even more pronounced along the ΓK direction and will be discussed in the next section.

The ΓM spectra show for $\vartheta \geqslant 22°$ that the t_{2g}-related emission consists of two individual substructures, the lower one of which loses intensity for larger angles of electron incidence and seems to disappear completely between 29° and 32°. This can be interpreted as the crossing of the metallic d_{z^2}-derived band through the Fermi energy. The point of intersection is in good agreement with the value of k_F determined from ARPES, where the occupied part of the d_{z^2} band was observed [5, 7]. The ARPES spectra also showed a non-dispersing structure close to E_F, which is possibly an 'impurity' state due to self-intercalated excess vanadium atoms. From the ARIPES data there is no hint for any such localized states in the unoccupied energy range. The shape of the t_{2g} peak on the low-energy side in the $\vartheta < 17°$ spectra may be due to a Se 4p-derived hole pocket around the Brillouin zone centre, which was inferred from recent ARPES data on VSe_2 [18].

Concerning the e_g emission we find marked differences between the intensities of the ΓM and ΓM′ spectra. While along the ΓM′ direction this structure becomes very pronounced for $\vartheta \geqslant 20°$ and shows for some angles a substructure, which allows us to resolve the d_{xz}- and d_{yz}-derived bands, its intensity almost breaks down along ΓM and is recovered only for $\vartheta > 40°$. Such intensity variations have been observed for all studied 1T-TMDCs. Similar effects were observed also for the photoemission Ta d-band intensities from 1T-TaS_2 and 1T-$TaSe_2$ [19] and explained as a shadowing effect due to the opaqueness of the neighbouring chalcogen atom for the escaping photoelectron. However, from our data and the geometry of our experiment we can rule out such a shadowing hypothesis (for a fuller discussion see [16]). Rather, the observed trigonal symmetry in intensity has to be attributed to the transition matrix element describing the excitation (de-excitation) process in ARPES (ARIPES). From their ARIPES data on 1T-VSe_2, Law *et al* [8] arrive at the same conclusion.

Apart from the intensity asymmetry there appears to be no significant difference between the ΓM and ΓM′ spectra concerning peak energies and dispersions. This is not a trivial observation, because a strict sixfold symmetry of the band structure is only to be expected if the three-dimensional electron wavevector lies either in the base plane (ΓKM) or in the top plane (AHL) of the Brillouin zone. Thus, considering the indeterminacy of the wavevector component perpendicular to the layers ($k_\perp$) the overall agreement of the experimental energies and dispersions in the ΓALM and ΓAL′M′ half-planes can be traced back to the two-dimensionality of the electronic structure of this layered material.

Along the ΓK direction the t_{2g} manifold displays some substructure between $\vartheta = 30°$ and 40°, where the lower (d_{z^2}) band moves a little away from the rest of the emission and reduces slightly in intensity. As opposed to the behaviour along ΓM this band does not seem to intersect the Fermi level, but at 60° merges again in the upper t_{2g} bands. The e_g manifold remains clearly observable in all ΓK spectra and can for ϑ between 30° and 50° be resolved into its two components.

Among the existing band-structure calculations we found best correspondence between experiment and theory for the self-consistent (non-muffin-tin) LCAO calculation

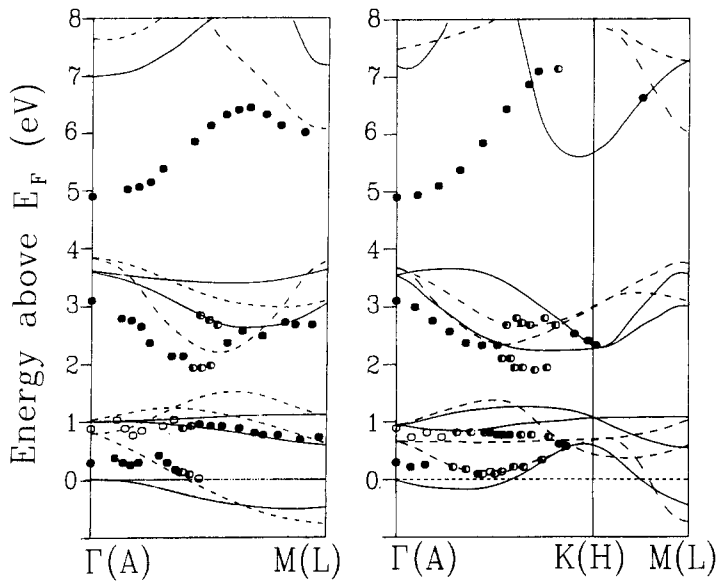

Figure 2. Experimental conduction band structure within (*a*) the ΓALM and (*b*) the ΓAHK half-planes compared with the calculation of Zunger and Freeman [2]: ●, strong ARIPES features; ○, weak ARIPES features; ——, theoretical bands within the basal (ΓKM) plane of the Brillouin zone; – – –, theoretical bands within the top (AHL) plane of the Brillouin zone.

of Zunger and Freeman [2] concerning both the energy and the dispersion of the unoccupied bands. Less satisfying agreement was found for the calculations in [1, 3]. Apart from the not well reproduced band energies the augmented plane-wave calculation of Myron [3] overestimates the dispersion of the V 3d states. To a minor extent this also applies to the layer method calculation of Woolley and Wexler [1], which additionally predict the e_g bands about 1 eV too low in energy.

In figure 2 our experimental conduction band structure is shown in comparison with the result of the calculation of Zunger and Freeman along the ΓM(AL) and ΓK(AH) directions. Along ΓM we find the emission due to the upper t_{2g} bands well reproduced by the theory. Concerning the lower t_{2g} band (i.e. the d_{z^2}-derived band) the calculation predicts it almost completely occupied along ΓM apart from a tiny hole pocket around the Γ point. However, in the ARIPES spectra this band can be followed up to almost $\frac{1}{2}$ΓM(AL), so that its experimental dispersion resembles much more the calculated dispersion along the AL line. The experimentally determined energy of the e_g bands is about 0.5 eV lower than calculated, but their dispersions are reasonably well reproduced. Along the ΓK (AH) direction similar agreement is observed. The experimental d_{z^2} band is almost dispersionless and seems to remain entirely unoccupied along this direction. Again, this resembles more the theoretical band along the AH line than along ΓK, where the calculation finds large parts of the band to be occupied. The dispersion of the e_g bands follows nicely the theoretical dispersion although slightly lower in energy.

The experimental band structure derived from our data agrees very well with the ARIPES results of Law *et al* [8]. Both studies find their experimental bands best described by the theoretical band structure in [2] within the AHL plane rather than the ΓKM plane. On the other hand, since both experimental $E(k_{\|})$ band structures have been

measured with distinctly different photon energies (20 eV in [8]; 9.88 eV in this work), they have necessarily mapped different parts of the three-dimensional Brillouin zone owing to the different values for $k_\perp$. From this fact and from the agreement of both experimental studies, two conclusions can be drawn: the $k_\perp$-dispersion must be smaller than calculated by Zunger and Freeman, and the theoretical band structure in the ΓKM plane should follow more closely the bands within the AHL plane.

4. Image potential state

We have not yet discussed the structure in the spectra in figure 1, which is located at almost 5 eV above E_F for normal incidence. It disperses upwards along ΓM up to 6.4 eV and turns down again to 5.9 eV towards the zone boundary. Along ΓK a parabolic dispersion can be followed to even larger angles until it levels off at about 7 eV near the K point. As can be seen from figure 2 there is obviously no theoretical counterpart for this structure in the calculation of Zunger and Freeman, but it is rather situated in the volume band gap between the e_g manifold and the antibonding σ^* states. The latter have been observed as a broad feature centred at about 8 eV with a threshold at about 6.5 eV by Law *et al* [8]. They also observed the 5 eV peak at normal incidence and found it to be non-dispersing along ΓA from their photon energy-dependent ARIPES data, which suggests an explanation as a surface state. Indeed, a similar peak has been observed for $TiTe_2$ and $TiSe_2$ [15] and was interpreted as an image potential state (IPS). Such a state can occur in a metal if the vacuum level lies in a gap of the projected volume band structure. In that case an electron directly in front of the surface cannot penetrate into the bulk and becomes trapped by the potential of its own image charge, giving rise to a Rydberg-like series of energy terms, which in a simple approximation can be written as

$$E_n(k_\parallel) = -0.85\ \text{eV}/n^2 + (\hbar^2/2m^*)k_\parallel^2 \qquad n = 1, 2, 3, \ldots$$

with respect to the vacuum level. The second term describes the kinetic energy parallel to the surface with an effective band mass m^* [20, 21].

Because Law *et al* assumed a work function of 4.4 eV taken from [5], they had to rule out an interpretation of the 5 eV peak as due to an IPS. As already discussed in section 2, there are good arguments that the work function of 5.76 eV determined in this work represents the correct value. Using this work function and the observed energy of nearly 5 eV yields a binding energy with respect to the vacuum level of 0.82 eV in very good agreement with the predicted value of the $n = 1$ IPS. The higher-order terms of the Rydberg-like series are beyond the resolution of our ARIPES spectrometer.

As seen in figure 2, towards larger $k_\parallel$ the IPS deviates from the expected parabolic dispersion and flattens (along ΓK) or even disperses down again (along ΓM). This behaviour is not contained in the simple theory mentioned above but can be understood from a resonance or even hybridization of the surface state with the underlying bulk bands. Indeed, along ΓM (AL) the IPS seems to follow the calculated dispersion of the lowest σ^*-like volume band (figure 2(*a*)) along the AL line. For the ΓK direction the IPS does not appear to interfere with the theoretical σ^* band along the ΓK line (figure 2(*b*)), being consistent with the observation that all experimental bands tend to follow the theoretical dispersions in the AHL plane rather than in the ΓKM plane. The hybridization of the IPS with the volume bands also nicely explains its broadening towards larger angles of incidence (figure 1).

In order to obtain effective band masses parabola have been fitted to the $E(k_\parallel)$ data of the IPS around the Γ point yielding $m^* = 1.3 \pm 0.2m_0$ for the ΓM and $1.15 \pm 0.1m_0$

for the ΓK direction. The enhancement of the band masses has been under debate for some time [21] and may at least in part be understood from the interaction of the IPS with the bulk bands. It can be shown in a more elaborate theory [22] that the effective mass of the IPS increases as the size of the volume gap and the separation of the IPS from the upper volume bands becomes smaller. This explains the higher band mass along ΓM, where the IPS leaves the bulk band gap already at 6 eV, while along ΓK it disperses to higher energies until it merges into the projected volume band structure above 7 eV.

5. Conclusion

We have presented a mapping of the unoccupied bandstructure of 1T-VSe_2 by means of ARIPES. The spectra reveal the splitting of the V 3d states into bands of t_{2g} and e_g character. The lowest t_{2g} band is seen to disperse through the Fermi level along the ΓM (AL) direction in agreement with corresponding ARPES data. In the comparison of our results with the band-structure calculation of Zunger and Freeman we find as a general tendency the experimental bands best described by the theoretical dispersions within the top (AHL) plane of the Brillouin zone. We find also good correspondence to the ARIPES data of Law *et al*. The agreement between both ARIPES studies despite the different photon energies used suggests a lower overall $k_\perp$-dependence of the three-dimensional electronic structure than theoretically predicted, thus confirming the result of photon energy dependent normal incidence ARIPES by Law *et al*. The determination of the work function by TCS yields a value similar to those obtained from other TMDCs and allows an ARIPES peak at 5 eV for normal incidence to be consistently interpreted as an image potential state.

References

[1] Woolley A M and Wexler G 1977 *J. Phys. C: Solid State Phys.* **10** 2601
[2] Zunger A and Freeman A J 1979 *Phys. Rev.* B **19** 6001
[3] Myron H W 1980 *Physica* B **99** 243
[4] Hughes H P, Webb C and Williams P M 1979 *J. Phys. C: Solid State Phys.* **12** L173
[5] Hughes H P, Webb C and Williams P M 1980 *J. Phys. C: Solid State Phys.* **13** 1125
[6] Drube W, Karschnick G, Skibowski M, Thies R and Völkert K 1980 *J. Phys. Soc. Japan Suppl.* A **49** 137
[7] Anderson O 1986 *Doctoral Thesis* University of Kiel
[8] Law A R, Andrews P T and Hughes H P 1990 *Vacuum* **41** 553; 1990 *J. Phys.: Condens. Matter* submitted
[9] Babbe N, Drube W, Schäfer I and Skibowski M 1985 *J. Phys. E: Sci. Instrum.* **18** 158
[10] Schäfer I, Drube W, Schlüter M, Plagemann G and Skibowski M 1987 *Rev. Sci. Instrum.* **58** 710
[11] Carstensen H, Claessen R, Manzke R and Skibowski 1990 *Phys. Rev.* B **41** 9880
[12] Straub D and Himpsel F J 1986 *Phys. Rev.* B **33** 2256
[13] Claessen R, Carstensen H and Skibowski M 1990 to be published
[14] Claessen R 1990 unpublished
[15] Drube W, Schäfer I and Skibowski M 1987 *J. Phys. C: Solid State Phys.* **20** 4201
[16] Claessen R, Burandt B, Carstensen H and Skibowski M 1990 *Phys. Rev.* B **41** 8270
[17] In agreement with Law *et al* and other workers we define the ΓM (ΓM′) direction as that in which the first neighbouring Se atom lies beneath (above) the ΓM line
[18] Johnson M T, Starnberg H I and Hughes H P 1986 *J. Phys. C: Solid State Phys.* **19** L451
[19] Smith N V and Traum M M 1975 *Phys. Rev.* B **11** 2087
[20] Echenique P M and Pendry J B 1978 *J. Phys. C: Solid State Phys.* **11** 2065
[21] Smith N V 1988 *Rep. Prog. Phys.* **51** 1227, and references therein
[22] Smith N V 1985 *Phys. Rev.* B **32** 3549